SLAC-PUB-12109
September 2006

PHOTOELECTRON EMISSION STUDIES IN CsBr AT 257 nm

Juan R. Maldonado[1], Zhi Liu*, Yun Sun*, Piero A. Pianetta* and Fabian W. Pease
Electrical Engineering Department, Stanford University, Stanford, CA 94305
*Stanford Synchrotron Radiation Laboratory, Menlo Park, CA 95025

ABSTRACT

CsBr/Cr photocathodes were found [1,2] to meet the requirements of a multi-electron beam lithography system operating with a light energy of 4.8 eV (257nm). The fact that photoemission was observed with a light energy below the reported 7.3 eV band gap for CsBr was not understood. This paper presents experimental results on the presence of intra-band gap absorption sites (IBAS) in CsBr thin film photo electron emitters, and presents a model based on IBAS to explain the observed photoelectron emission behavior at energies below band gap. A fluorescence band centered at 330 nm with a FWHM of about 0.34 eV was observed in CsBr/Cr samples under 257 nm laser illumination which can be attributed to IBAS and agrees well with previously obtained synchrotron photoelectron spectra[1] from the valence band of CsBr films.

I. Introduction

Previous studies for multi electron beam mask writer applications [1,2] demonstrated the successful operation of CsBr photocathodes at 257 nm and high current density. Differing from reference [3], we postulated that a Cs rich surface and UV induced intra-band gap absorption sites (IBAS) were responsible for the relatively large photoelectron yield observed after exposure at 257nm (4.8 eV) in CsBr photocathodes. In this paper we have assumed a single crystal band gap of about 7.3 eV[4] for our CsBr films on Cr coated sapphire substrates. This assumption is based on earlier work[3] on CsBr films depositeds on Au and Cu substrates found to be crystalline. The experimental results and model presented in this paper substantiates the presence of IBAS in CsBr/Cr films and their influence on photoelectron emission below the band gap.

II. Experimental Procedure

The experiments were performed in the system for photoelectron emitter studies referred to as the Source Development Test stand (SDT) in other publications[1], recently installed in the Stanford Synchrotron Radiation Laboratory at the Stanford Linear Accelerator Center (SLAC). Single crystal c-

[1] Mailing address:
Stanford Synchrotron Radiation Laboratory, SSRL/SLAC
2575 Sand Hill Rd. MS69
Menlo Park, CA 94025

Presented at 50th International Conference on Electron, Ion and Photon Beam Technology and Nanofabrication, 5/30/2006-6/3/2006, Baltimore, MD, USA

Work supported in part by Department of Energy contract DE-AC02-76SF00515

axis sapphire substrates about 1cm x 1cm x 0.5 mm were patterned with an array of 15 um wide 80 nm thick Cr bars. The patterned sapphire substrates were cleaned and then e-beam evaporated with a 5 nm thick Cr film. They were subsequently coated at ~1x10E-9 torr with a 15 nm film of CsBr utilizing an MBE-Komponenten effusion cell at ~ 400 ^{o}C.

III. Experimental Results of light transmission through the CsBr Film

The CsBr film was irradiated with 257 nm laser light at powers ranging from 10-40 mW with an optical system shown in Fig. 1A at a vacuum pressure < 10^{-10} torr. The laser beam was expanded and focused on the CsBr films to a 1.5 micron spot with a quartz UV lens resulting in an inferred photo current density greater than 100 A/cm^2. The UV transmitted light thru the CsBr film was measured simultaneously with the generated photocurrent. Only a portion of the transmitted light is collected by the detector because the beam spreads after focusing on the sample by the lens and no lens is utilized in front of the detector as shown in Fig 1A. The results presented in Fig 1B indicate the correlation between the transmitted light and the incident laser power on the film. We observe from the figure that the ratio of the transmitted light to the incident light decreases with increasing laser power. This ratio indicates the opacity or increased absorption induced in the films by the IBAS formation. Furthermore, Fig. 1C indicates the correlation between the photoelectron yield and the light transmission in the film which is consistent with IBAS formation: The photoelectron yield increases when the light transmission decreases and vice versa. Color center bands in CsBr which may be related to the observed light absorption have been reported [5] in the past and are investigated in this paper.

IV. Experimental results utilizing fluorescence from the CsBr film

The goal of these experiments is to detect the fluorescence caused by electronic transitions amongst IBAS (that may already be present, induced or populated by the 257nm radiation) in the CsBr film. Using the system described below, we have identified a fluorescence band around 330 nm in CsBr which can explain the observed photoemission at incident light energies below the band gap.

An Ocean Optics Model 2000 spectrophotometer was utilized to detect the fluorescence from the IBAS as shown in Fig. 2A and a series of experiments were performed with the CsBr sample both in the reflection and transmission modes described in Figs. 2B & 2C. In the reflection mode, the 15 nm CsBr film is illuminated with the 257nm laser focused through the CsBr film on one of the 15 um wide Cr bars located under the film. The reflected light from the Cr bar travels back through the CsBr film and the focusing lens as shown in Fig. 2A and is detected by the spectrophotometer. In the transmission mode, the CsBr sample is turned over and illuminated through the sapphire substrate plate between two Cr bars as shown in Fig. 2C. The fluorescence signal developed in the CsBr film is detected through the focusing lens as shown in Fig. 2A.

Due to dispersion in the focusing UV quartz lens, the focal length is wavelength dependent. Therefore, the focal plane of the incident 257nm light differs from the focal plane of the fluorescent signal developed in the film. Since the reflected 257nm signal is developed at the focal plane, the focused 257nm beam reflected from the Cr bar and transmitted back through the focusing lens is collimated when it reaches the optic fiber. However, any fluorescent beam at a wavelength different than 257nm is not collimated (diverges) on the optic fiber when the incident 257nm beam is focused on the film. To maximize the fluorescent signal, the focusing lens is moved away from the film enough to correct for the focal distance difference at the fluorescence wavelength. However, this causes the 257nm incident beam to be out of focus on the CsBr film. This effect is not too important since the goal of the experiment is to detect the fluorescence signal. In future experiments, we plan to correct for this effect with an auxiliary lens located after the 257nm mirror shown in Fig 2A. This arrangement can allow independent foci for the 257nm and the fluorescence signal.

Experiments in the Reflection Mode

In these experiments, the cathode is illuminated in the reflection mode as shown in Fig 2B. The 257nm light illuminates the CsBr film from the same side as the electrons are collected. The effective thickness of the CsBr film is 2X in this mode since the light is reflected back into the film by the Cr

bars deposited on the sapphire substrate. This mode of operation was chosen for the first experiments because it can increase the total absorption of 257nm light, and therefore the IBAS fluorescence signal relative to the transmission mode. However, the fluorescence signal was also observed in the transmission mode as shown below with good signal to noise ratio. To improve the fluorescence signal to noise ratio, the spectrometer's detector is located behind the final projection lens as shown in Fig. 2A. Due to the lens collimation effect described above, this arrangement enables us to collect the fluorescence light from a larger solid angle by defocusing the final UV lens as mentioned above.

Results obtained with the laser beam focused on the CsBr film did not produce a strong fluorescence signal. Due to optical system losses, the actual 257nm light reaching the CsBr was about 50% less than the output laser power. At 60 mW output laser power, the spectrum indicated the presence of three peaks: a sharp peak at 257nm, and two broad peaks at 280nm and 480nm. A very small extra peak at ~330nm was buried in the noise as shown in Fig. 3A. The 280nm and 480 nm peaks were identified as fluorescence peaks emanating mainly from the quartz optic fiber.

If the final objective lens is moved away from the sample by about 1mm to get closer to the focal plane of the fluorescence signal, a new peak at ~330nm appears shown in Fig. 3B with FWHM of about 0.34 eV . Calculations of the expected shift of the focal plane from 257nm to 330 nm for the fused silica SDT UV lens indicate a value of 1.88 mm..

To confirm the generation of the fluorescence peak from the sample, we measured the behavior of the four peaks varying the lens distance to the sample. The normalized peak areas of 257nm, 280nm and 480nm followed each other (oscillating) as the lens is moving away from the sample as shown in Fig. 3C. Detecting the signal directly with the spectrophotometer without the optic fiber it was found that the 280nm and 480nm peaks were generated mainly by the 257nm radiation on the optical fiber. On the other hand, the peak intensity at 330nm increased monotonically within the maximum range of defocusing as shown in Fig. 3C. This shows that the 330nm peak is not generated by fluorescence

from the optical components in the optical path away from the focusing lens, but emanates from the sample.

Normalizing the 334nm signal to the input laser power as shown in Fig. 4A, it is possible to obtain a relative quantity for the efficiency of production of the 334nm signal. This is equivalent to the efficiency of creating or populating IBAS by the 257nm incident beam.

It appears from Fig. 4A that the efficiency of 334nm production in CsBr increases with low laser power and remains fairly constant after about 30 mW laser power (15 mW on the sample). This is consistent with the observed activation[1] of the CsBr photoemitters at 257nm, and the light absorption behavior with laser power of CsBr at 257 nm. We have shown above that the light absorption in the film increases with 257 nm incident power. Therefore, it appears from Fig. 4A, that the population or formation of IBAS have reached some equilibrium for >30 mW laser power.

Data shown in Fig. 4B taken a few days later in another area (after several different runs in other adjacent areas lasting more than 20 hours at several power densities), indicates that the fluorescence efficiency did not vary appreciably with laser power. This may be due to the fact that the film had been UV exposed over a large adjacent area by repeated defocusing experiments, and the data shown in Fig. 4A is only valid during the initial exposure of a virgin area. More work is needed to shed light on the variation of fluorescence efficiency with laser power.

Experiments in the Transmission Mode

In this mode of operation the CsBr sample is illuminated through the sapphire substrate plate. The results for the 257nm focused beam at 30 mW laser power are shown in Fig. 5A. The data was obtained after irradiation for less than 1 hour at 30 mW laser power. We observe that the 330 nm peak is relatively small compared with the quartz fluorescence peak at 280nm when the beam is focused on the sample. In other experiments, the 330 nm peak appears to be present from the beginning of the irradiation at low laser power (5-10 mW). Therefore, it is not clear if it was induced by the 257 nm radiation in a very short time (<1 sec), or if it was already present in the deposited CsBr film. More

experiments are needed to clarify this behavior which may have implications for future improvements in alkali halide photoemitters.

The data shown in Fig. 5B was obtained with the focusing lens moved away about 1 mm from the focal plane at 257nm. This position is closer to the focal plane at 330nm, and enhances the 330nm relative to the quartz fluorescence peak at 280 nm as mentioned above. The behavior of the intensity and the fluorescence efficiency of the 330 nm peak for a fully activated [1] sample in the transmission mode is similar to the results presented above obtained in the reflection mode. The 257nm, 280nm and 480nm peaks show a similar behavior which differs from the 330nm peak. We observed very little change in the fluorescence efficiency with laser power in the transmission mode with the beam defocused.

The following experiment was performed to study the effect of pressure on the photoelectron yield and IBAS in CsBr in the transmission mode. The results shed some light on the degradation mechanism of the CsBr. The data shown in Fig. 5C was obtained at a base pressure of 8E-11 torr. The corresponding data obtained when the CsBr sample was subjected to a 3×10^{-8} torr burst is shown in Fig.5D.

From the intensity profiles we conclude that surface contamination was localized at the activated region, the unactivated region was not affected by the pressure burst. The activated surface is more vulnerable than the unactivated surface, probably due to photolysis caused by the UV radiation and contamination of the Cs rich area of the illuminated spot by the reaction by-products. The data indicate that after the sample was exposed to a 3×10^{-8} torr burst, the photoelectron yield dropped from 130nA/mW to 110nA/mW. After the vacuum recovered, the photoelectron yield also recovered which is consistent with UV light surface cleaning by photolysis. However, there was very little change on the intensity of the 330 nm fluorescence signal with exposure to high pressure. This indicates that the IBAS fluorescence centers are not affected by the pressure jump and they may be

localized in the bulk away from the surface. The fact that the normalized fluorescence yield does not change very much with power in both low and high pressure cases agrees well with previous data.

Correlation between Photoelectron yield and 330nm peak

The correlation of the photoelectron yield with the 330nm peak during operation is shown in Fig. 6A. Data was obtained over a 100 hour period at 21 mW incident power on the sample (40 mW laser power). Both the fluorescence intensity and the photocurrent degrade with time as shown in the figure. One mechanism of photoelectron yield degradation may be due to surface contamination caused by photolysis during UV exposure. This can prevent the formation of a Cs rich surface required to lower the work function. On the other hand, it is not likely that one or perhaps a few monolayers of contamination can cause enough absorption to decrease the 330nm fluorescence signal by more than 20% from the initial value as shown in Fig. 6A. The observed decrease of the fluorescence signal may be explained by the decrease in available states due to recombination. More work is needed to understand the observed behavior of the fluorescence degradation.

The effect of heating the CsBr sample from room temperature to about 90 ^{o}C is shown in Fig. 6B. The correlation between the photo current and the amplitude of the 330nm peak with increasing temperature is shown. There seems to be some sort of transition around 50 ^{o}C which is not understood. This may be related to some change in the material, and more work is needed to understand this behavior.

V. Model for photoemission

There are two mechanisms that contribute to the photoemission in CsBr. First, is the absorption of the 4.8 eV photons (257 nm) by the IBAS around 3.75 eV shown in Fig. 6C. Electrons occupying those states can acquire enough energy to reach the surface of the CsBr film. The second mechanism is the lowering of the work function by the migration of Cs to the surface. Experiments to substantiate a Cs rich surface after irradiation at 257nm were already reported [1]. This mechanism was shown to be time dependent and its effectiveness is subject to degradation by contaminants in the vacuum

system. The presence of oxygen appears to affect the lowering of the work function perhaps by disturbing a Cs dipole layer on the surface. It was observed during the pressure experiments, that the contamination due to photolysis by the UV radiation is local to the irradiated spot, and adjacent spots are not affected. These phenomena can be utilized to increase the lifetime of a large area CsBr photocathode by utilizing adjacent spots after degradation. It is also possible to utilize photolysis with UV irradiation to clean and rejuvenate a CsBr photocathode exposed to air for a short time.

The experimental results shown in Fig. 1C are consistent with our model. The increase in photoelectron yield and light absorption with illumination and vice versa indicate that a recombination mechanism may play a role. The incident UV light produces Cs migration to the surface (lowering the work function), and more electrons can escape the film. Fewer electrons will be recombined back to the IBAS. Therefore, the light absorption changes accordingly with illumination as more or less electrons leave the surface due to Cs migration as shown in Fig. 1C. At the same time, the density of states changes in the IBAS generated by the UV illumination may also contribute to this phenomenon.

Finally, the photoelectron spectra shown in Fig. 7A and 7B from the valence band of CsBr are consistent with the model and the location of the IBAS. We observe from Fig. 7B (an enlarged region of figure 7A indicating the data obtained inside the 7.3 eV band gap) that the 3.75 eV peak energy of the 330 nm fluorescence signal falls in the middle of the electron states recorded in the photoelectron spectra of the activated CsBr sample.

VI. Summary

We have observed a fluorescence band in CsBr films around 330 nm (~3.8 eV) with a FWHM of 30 nm (~0.34 eV). Assuming an energy gap in CsBr of about 7.3 eV, the presence of IBAS of about 3.8 eV may allow photoelectrons to reach and leave the Cs rich activated surface when irradiated with 257nm (4.8 eV) UV light. The IBAS appear to be in the “bulk” of the 15 nm film, and are not affected appreciably by surface contamination. It is not possible to infer from the data if the IBAS were created by the UV radiation or were already present in the CsBr films. More work is needed to clarify this

issue. However, the fluorescence efficiency data shows that the IBAS can be populated (excited states) by the 257nm radiation. The data is also consistent with previous [1] photoelectron spectroscopy studies that indicate Cs migration to the surface under 257nm UV irradiation. The combination of IBAS and the work function decrease due to Cs migration can explain the photoemission at light energy less than the bandgap of CsBr. In addition, the proposed model is also consistent with the changes in light transmission with illumination observed in the CsBr films and the photoelectron spectra from the valence band of CsBr. Finally, it must be remarked that the CsBr films are very robust and can be rejuvenated by the 257nm radiation after been exposed to contaminants in a relatively high pressure environment (~1E-8 torr).

References

1. Maldonado, J.R., S. Coyle, B. Shamoun, M. Yu, M. Gesley and Piero Pianetta et al., *Cs halide photocathode for multi-electron-beam pattern generator.* Journal of Vacuum Science and Technology B: Microelectronics and Nanometer Structures, **22**(6): p. 3025-3031 (2004).
2. J.R. Maldonado, S.T. Coyle, B. Shamoun. M. Yu, T. Thomas, D. Holmgren, X. Chen, B. DeVore, M.R. Scheifein and M. Gesley, Proc. SPIE 5220, 46, (2003).
3. T.H. DiStefano and W.E. Spicer, Phys. Rev. B, Vol. 7, No. 4, pp1554-1564, (1973).
4. F.C. Brown, C. Gahwiller, H. Fujita, A.B. Kunz, W. Scheifley, N. Carrera, Phys. Rev. B 2, 2126 (1970).
5. P. Avakian and A. Smakula, Phys. Rev., Vol. 120, No. 6, pp 2007-14, (1960).

Acknowledgements

This work was supported by a DARPA Grant F33615-00-1-1728 monitored by the Air Force office. We would like to thank Applied Materials for donating the SDT system to Stanford. Z. Liu would like to thank KLA-Tecor Co. for the support. Portions of this research were carried out at the Stanford Synchrotron Radiation Laboratory, a national user facility operated by Stanford University on behalf of the U.S. Department of Energy, Office of Basic Energy Sciences.

Figure Captions

Fig. 1. A) Schematic of the experimental arrangement in the SDT system at SSRL to study light transmission in CsBr films. **B)** Correlation between the CsBr film absorption (transmitted light) and incident laser power. The observed behavior is consistent with the formation of intrabandgap absorption sites by the UV irradiation. **C)** Observed **c**orrelation between the CsBr photoelectron yield (nA/mW top trace) and the normalized light transmission (A.U. bottom trace) for several incident laser powers (mW) shown in parenthesis. The photoelectron yield increases when more light is absorbed in the film, consistent with intrabandgap absorption site formation. The photoelectron yield data was averaged to reduce system noise.

Fig. 2. A) The main components of the SDT system optics and electronics. The photocathode sample is shown in the transmission mode. **B)** Reflection and **C)** Transmission modes of operation studied in the SDT system.

Fig. 3. A) Focused beam, 60mW laser power, 800ms CCD integration time, 20 Averages. *(Raw data minus the dark current background).* The fluorescence peaks from the optical fiber are observed. However, the 330 nm peak is buried in the noise. **B)** Two turn defocused beam, at 60mW laser power, 800ms integration time and 20 times average. The 330 nm fluorescence peak is observed after beam defocusing. C) Normalized peak area vs. defocus length plot. Curves B: 257nm, C: 480nm, D: 280nm and E: 330nm.

Fig.4. A) Efficiency of production of the fluorescence 334nm signal from the intraband states of CsBr obtained in the reflection mode with the beam defocused. B) Fluorescence efficiency vs laser power for CsBr sample after several days of laser experiments utilizing a defocused beam in reflection mode.

Fig.5. A) Transmission mode data for the focused beam case. Note that the 330nm peak is small relatively to the 280nm fluorescence quartz peak. **B)** Data obtained after defocusing the lens ~1 mm away from the focal plane at 257nm. The 330 nm peak increases as the focal plane of the fluorescence signal is approached. **C)** Photoelectron yield data obtained scanning the piezo electric flexure stage of the SDT system relative to the focused laser beam at a pressure of 8×10^{-11} torr. The photoelectron yield was recorded in an 80 μm field at 120 points along each scan line. The chrome bars and small square marks on the sapphire substrate are shown in black (low photoemission yield). The area where the laser hits the CsBr sample is shown as a bright spot. Intensity profiles along two perpendicular directions are also shown in the figure. **D)** Corresponding data obtained after the sample was subjected to a pressure burst of 3×10^{-8} torr.

Fig. 6. A) Correlation of photocurrent and fluorescence efficiency for a CsBr sample in transmission mode (TM) with time. **B)** Correlation of photocurrent and amplitude of the 330 nm fluorescence peak with increasing temperature at 40 mW laser power in TM . C) Model for photoemission below the band gap energy in CsBr. Electrons are photoemitted after UV absorption by the IBAS. The Cs layer which has been shown[1] to migrate to the surface with irradiation lowers the work function and increases the photoelectron yield. The electrons can return via the 5nm Cr film located under the CsBr film. The Fermi level of Cr is at 4.6 eV below the vacuum level and is shown to be within the IBAS.

Fig.7. A) Photo electron emission spectra from the valence band of CsBr obtained at 135 eV incident energy from the SSRL storage ring. B) Enlarged region from Fig. 7A indicating the region inside the 7.3 eV energy gap. The Fermi level of a test Au sample is shown for calibration purposes. The 330 nm (~3.8 eV) fluorescence band coincides with the electron states observed by photoelectron emission after white beam activation of the CsBr sample. The experimental results are consistent with the proposed model.

Experimental Arrangement

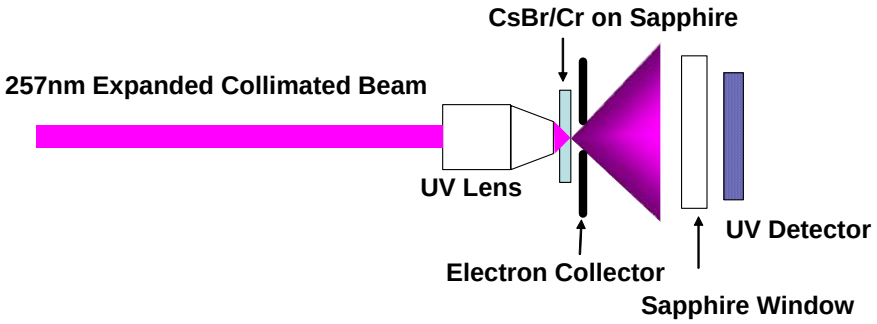

Beam Focused to ~1.5 micron spot

(A)

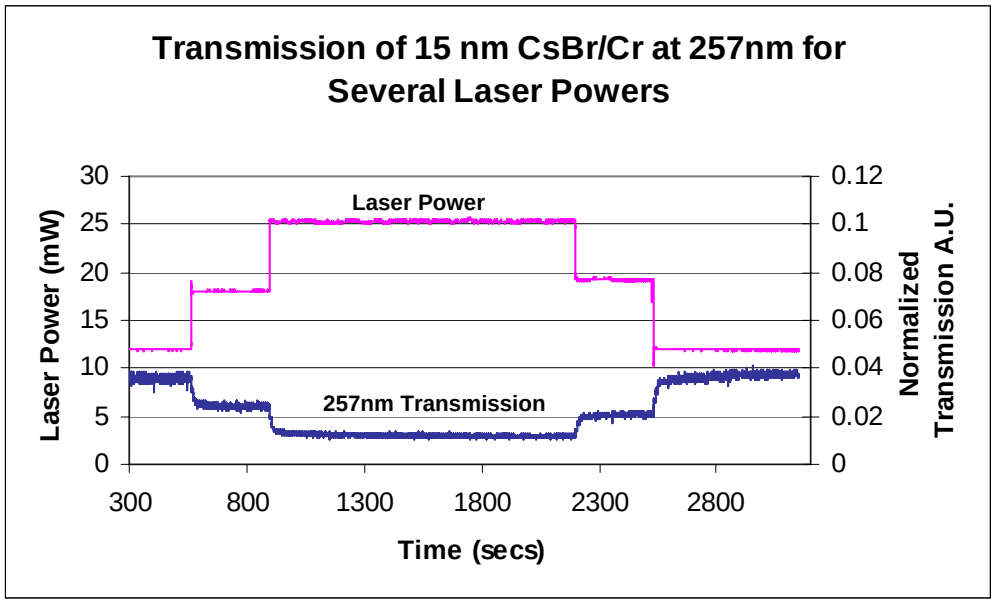

(B)

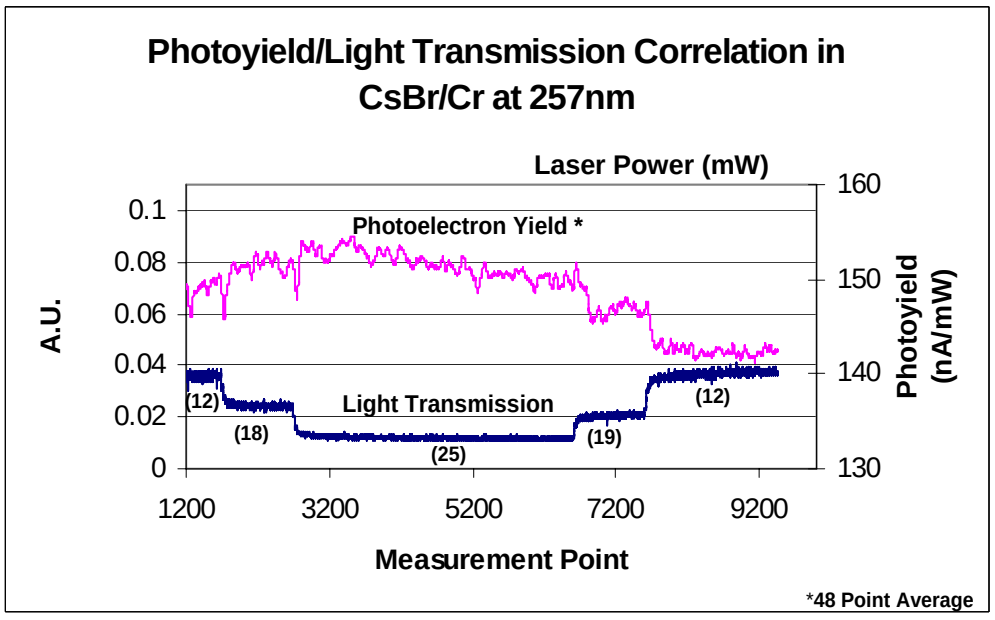

060104-155818rawdata-2.xls

(C)

SDT SYSTEM OPTICS FOR FLUORESCENCE MEASUREMENTS

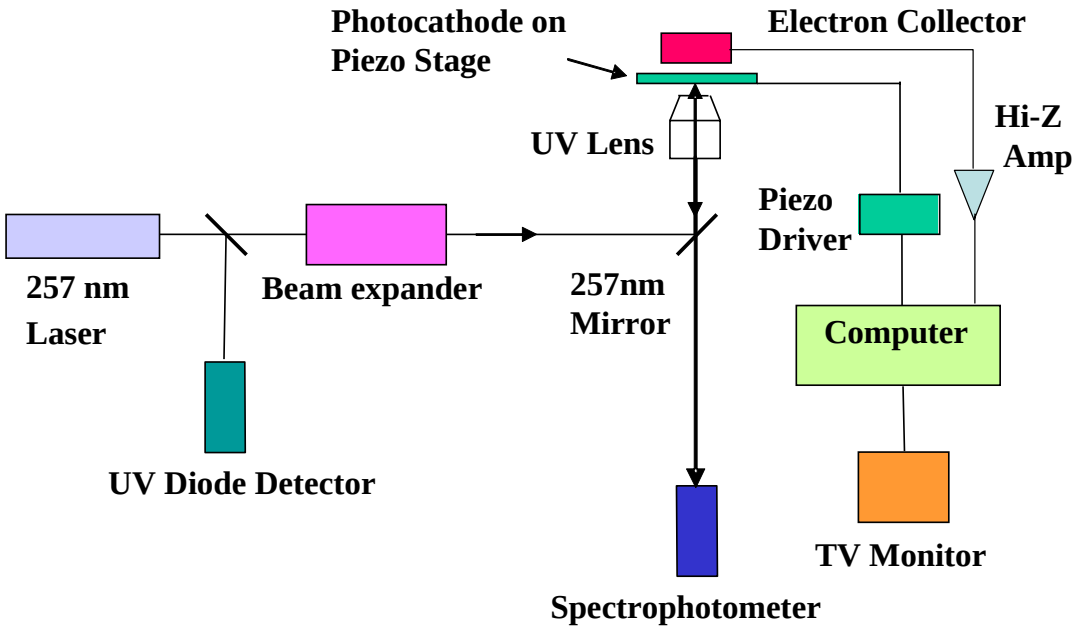

(A)

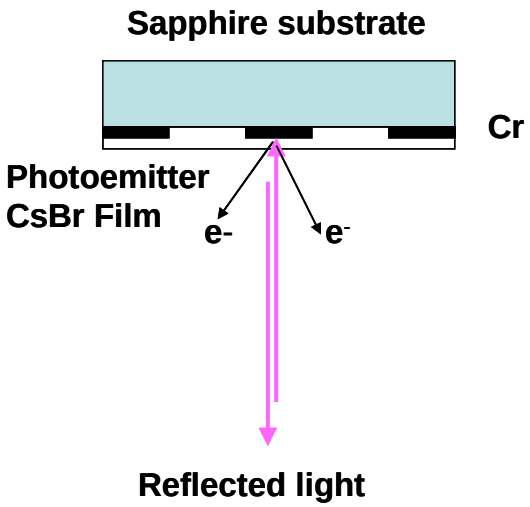

Reflection Mode

(B)

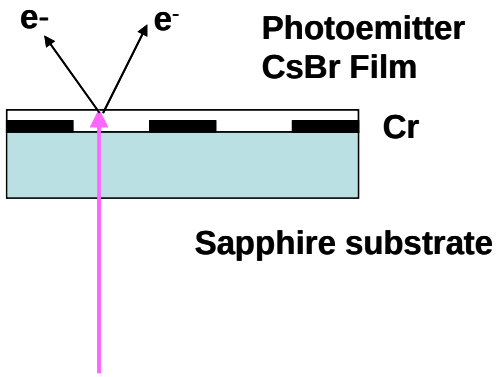

Transmission Mode

(C)

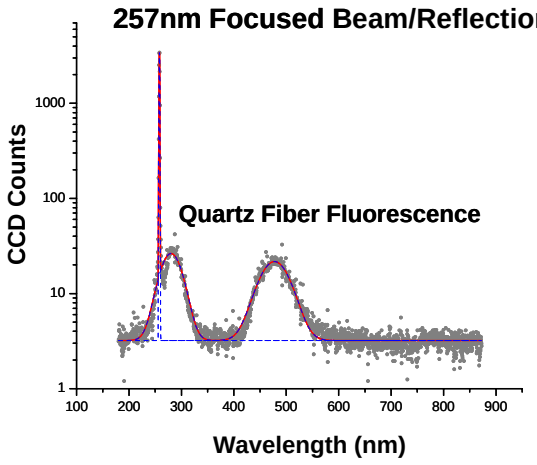
257nm Focused Beam/Reflection Mode
CCD Counts
Quartz Fiber Fluorescence
Wavelength (nm)

(A)

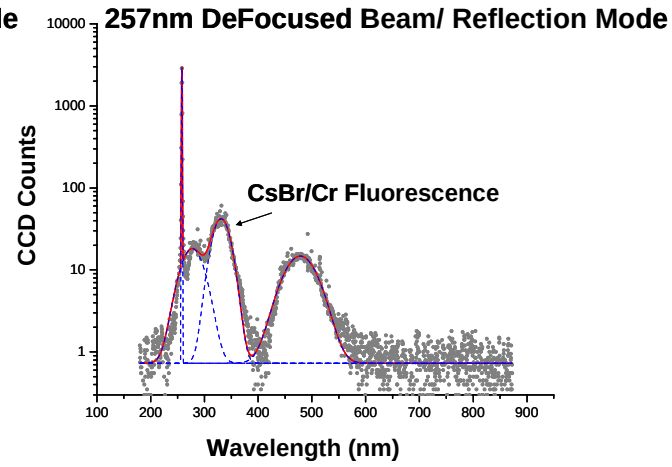
257nm DeFocused Beam/ Reflection Mode
CCD Counts
CsBr/Cr Fluorescence
Wavelength (nm)

(B)

(C)

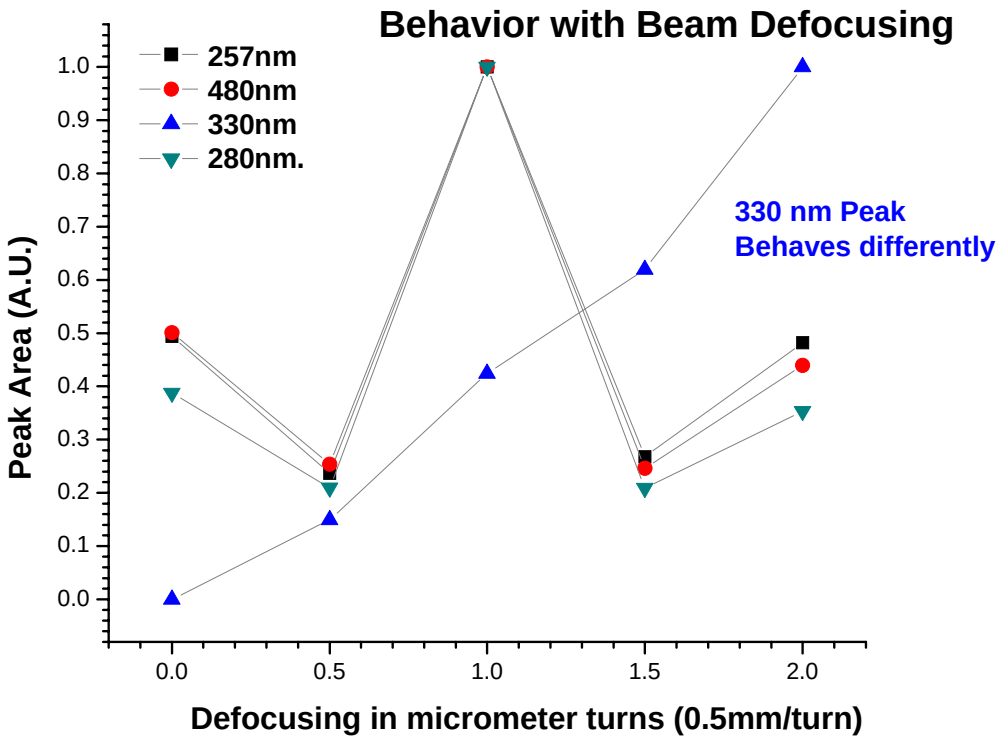
Behavior with Beam Defocusing
257nm
480nm
330nm
280nm.
330 nm Peak
Behaves differently
Peak Area (A.U.)
Defocusing in micrometer turns (0.5mm/turn)

(A)

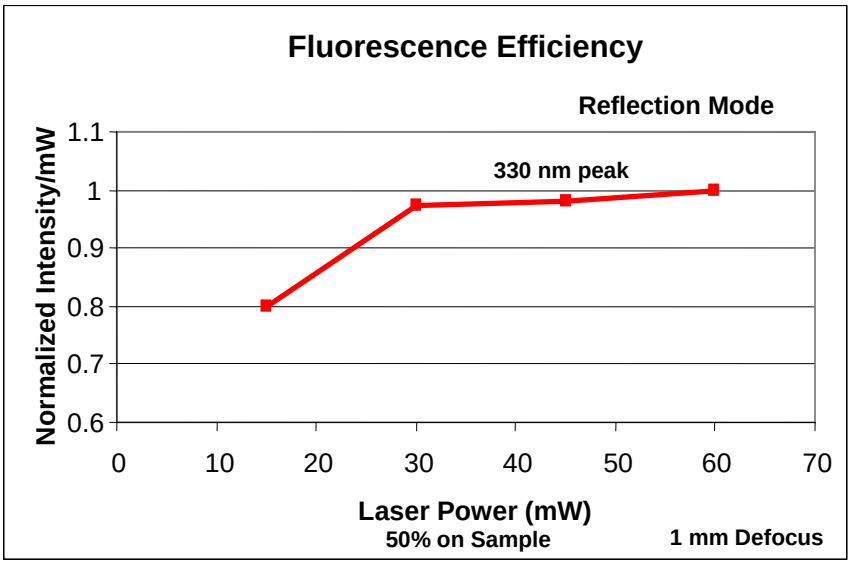
Fluorescence Efficiency
Reflection Mode
330 nm peak
Normalized Intensity/mW
1.1
1
0.9
0.8
0.7
0.6
0
10
20
30
40
50
60
70
Laser Power (mW)
50% on Sample
1 mm Defocus

(B)

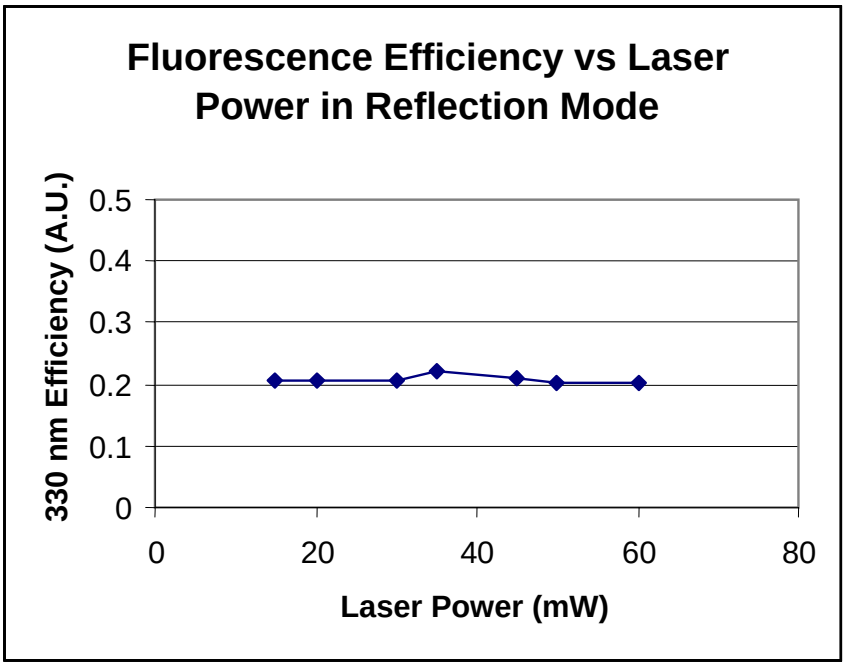
Fluorescence Efficiency vs Laser Power in Reflection Mode
330 nm Efficiency (A.U.)
0.5
0.4
0.3
0.2
0.1
0
0
20
40
60
80
Laser Power (mW)

(A)

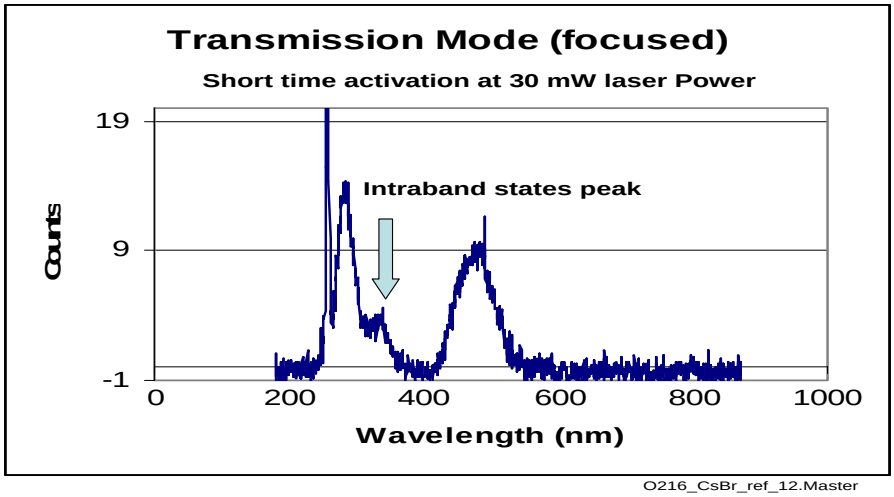
Transmission Mode (focused)
Short time activation at 30 mW laser Power
Intraband states peak
Counts
19
9
-1
0
200
400
600
800
1000
Wavelength (nm)
O216_CsBr_ref_12.Master

(B)

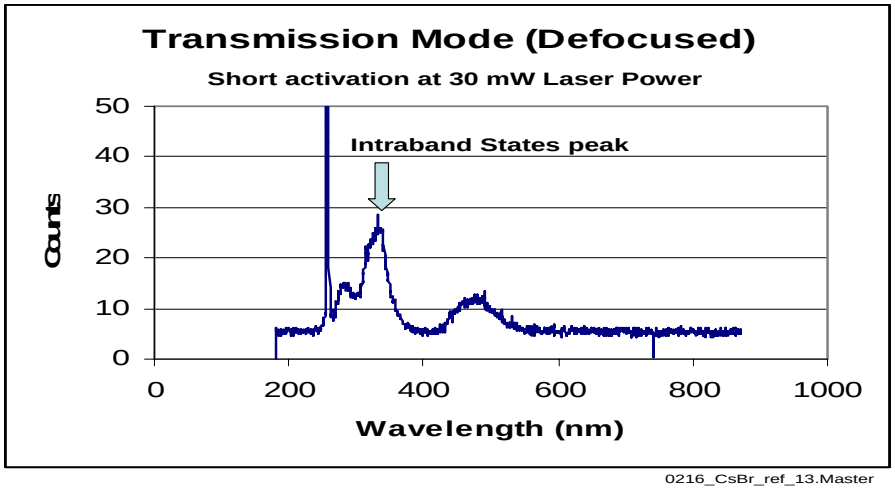
Transmission Mode (Defocused)
Short activation at 30 mW Laser Power
Intraband States peak
Counts
50
40
30
20
10
0
0
200
400
600
800
1000
Wavelength (nm)
0216_CsBr_ref_13.Master

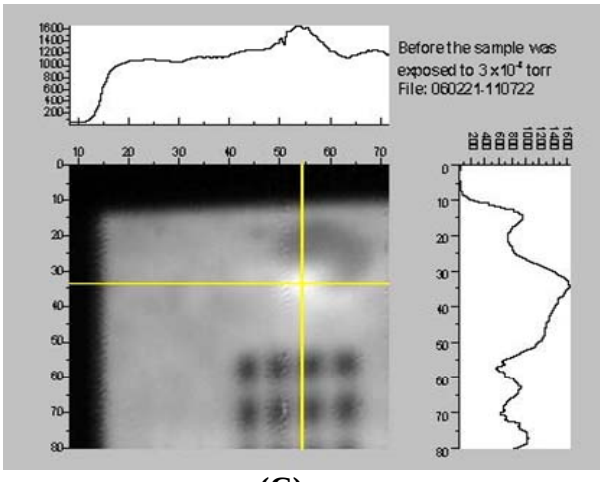
Before the sample was exposed to 3 x 10⁻⁴ torr
File: 060221-110722

(C)

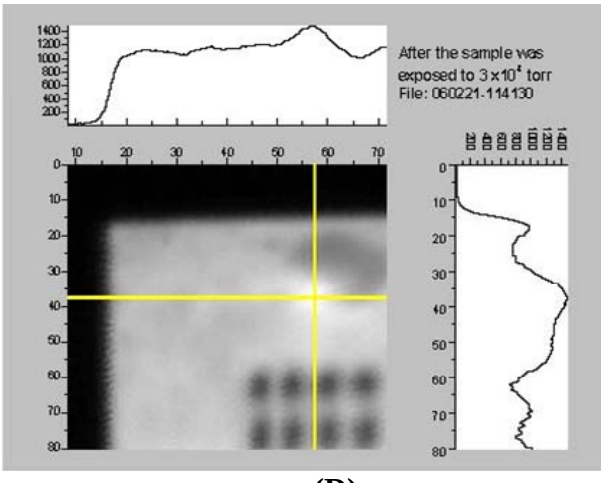
After the sample was exposed to 3 x 10⁻⁴ torr
File: 060221-114130

(D)

(A)

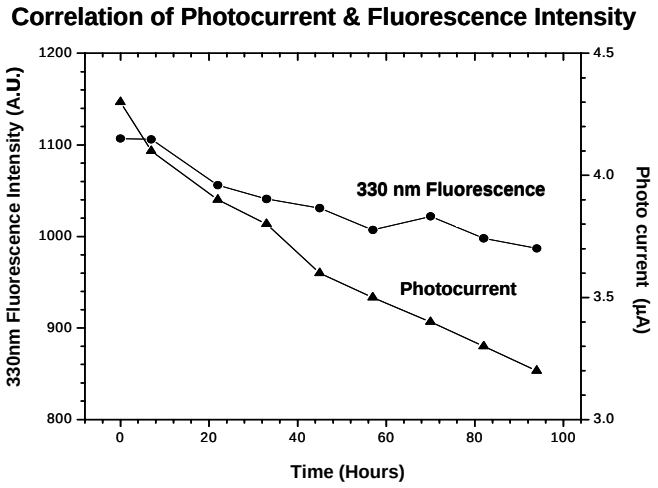
Correlation of Photocurrent & Fluorescence Intensity
330nm Fluorescence Intensity (A.U.)
Photo current (μA)
Time (Hours)
330 nm Fluorescence
Photocurrent
1200
1100
1000
900
800
4.5
4.0
3.5
3.0
0
20
40
60
80
100

(B)

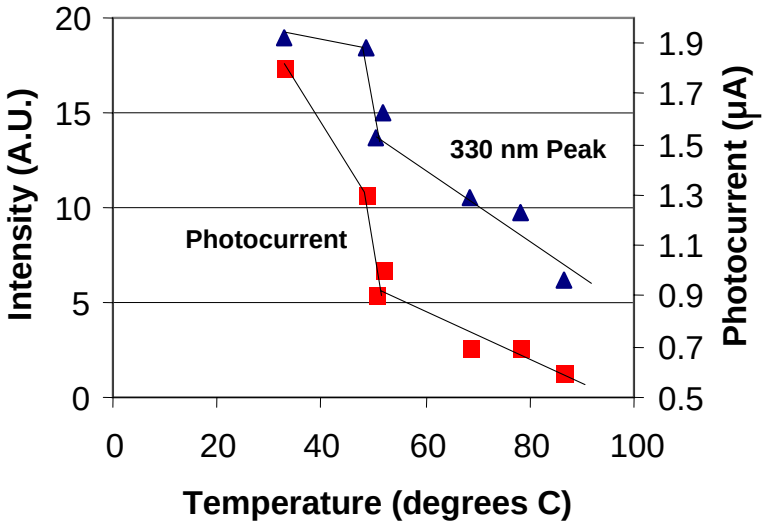
Correlation of Fluorescence & Photocurrent
Intensity (A.U.)
Photocurrent (μA)
Temperature (degrees C)
330 nm Peak
Photocurrent
20
15
10
5
0
1.9
1.7
1.5
1.3
1.1
0.9
0.7
0.5
0
20
40
60
80
100

(C)

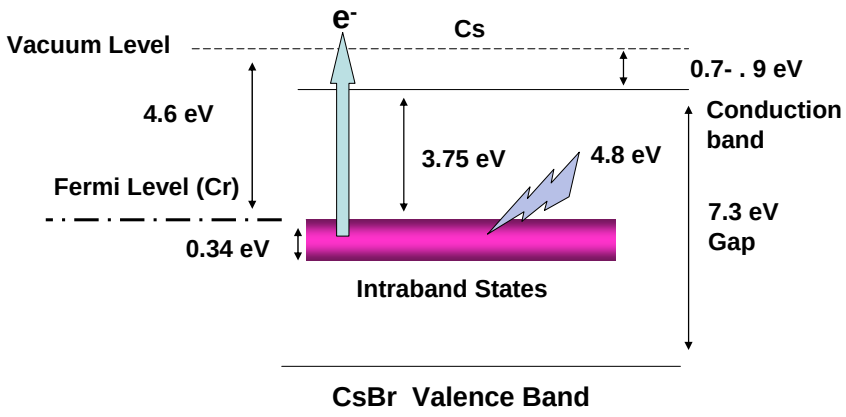
Model for Photoemission in CsBr at 257 nm
e-
Cs
Vacuum Level
0.7- . 9 eV
Conduction band
4.6 eV
3.75 eV
4.8 eV
Fermi Level (Cr)
7.3 eV Gap
0.34 eV
Intraband States
CsBr Valence Band

Photo Electron Emission Spectra from the Valence Band of CsBr

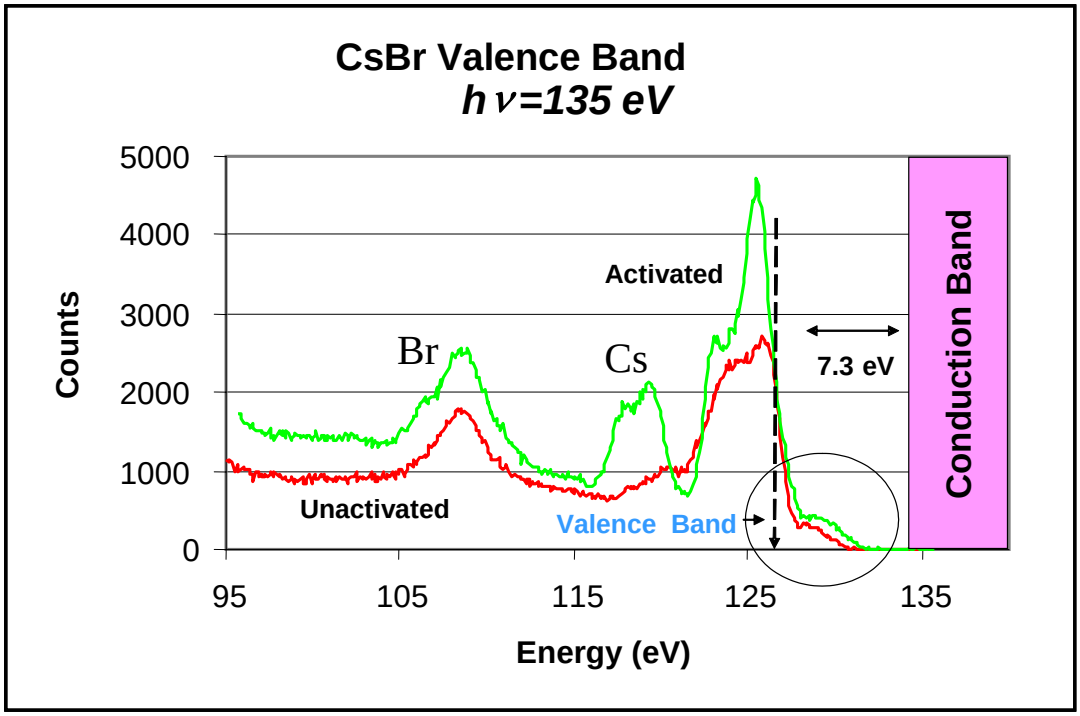

(A)

Photoelectron Spectra Consistent with Fluorescence Emission

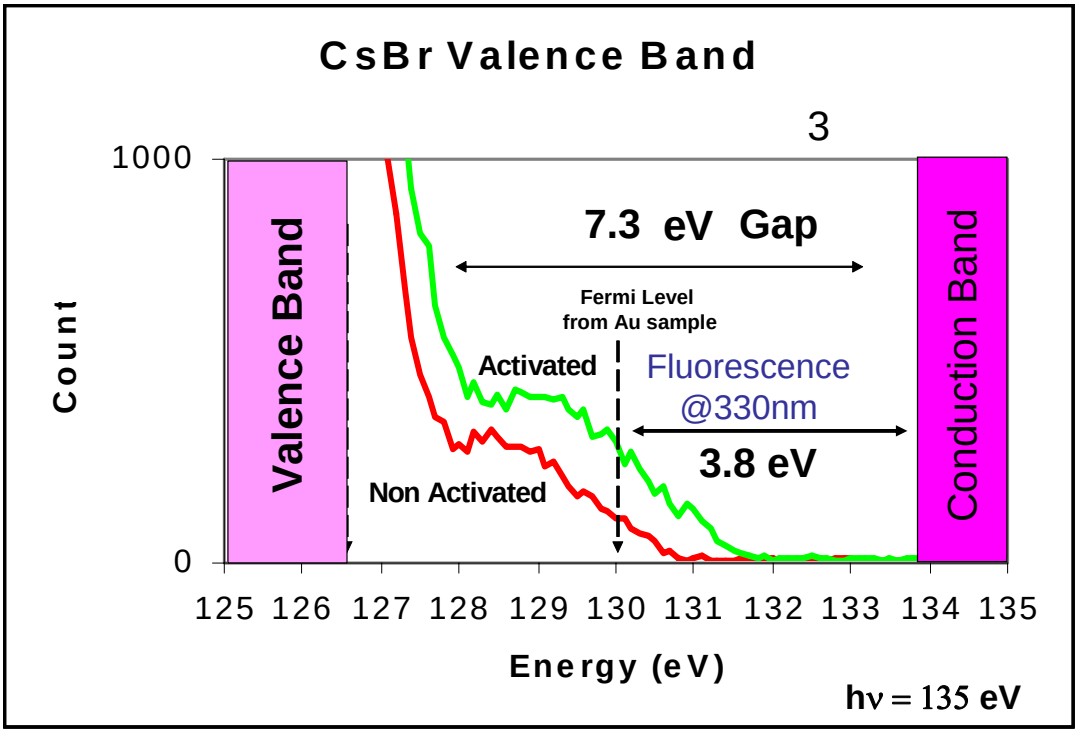

(B)